Numerical Simulation of Flow between Two Parallel Co-Rotating Discs

Dr. SMG. Akele[1] and Prof. J.A. Akpobi[2]

[1]Lecturer, Department of Mechanical Engineering Technology, Auchi Polytechnic, Edo State, NIGERIA

[2]Lecturer, Department of Production Engineering, University of Benin, Edo State, NIGERIA

[1]Corresponding Author: smg_sam2009@yahoo.com

ABSTRACT

     The study of fluid flow between two rotating discs aims to predict flow characteristics. In this paper numerical simulation is used to investigate axisymmetric swirling flow between two parallel co-rotating discs.

     Methodology entails, firstly, inputing parameters from CFD software are into previos study developed dimensionless radial velocity model for flow between two discs to obtain dimensional radial velocity of the model. Secondly, previous study parameters are used to perform numerical simulation on laminar and turbulent flows between two parallel co-rotating discs. The numerical simulation results are compared to previous study results. Then comparative numerical simulations was carried out on laminar and turbulent flows using CFD software.

     Results obtained showed that for the this study dimensional radial velocity and previous study dimensionless radial velocity, radial velocity distribution increase proportionately from the disc surface at 0m/s to 2208.00m/s and 0 to 0.0002396 respectively, at the domain centre. And both results satisfy initial inlet and boundary conditions with resultant parabolic profiles. In the study, it is shown that turbulent flow radial velocity profile is smoother than for laminar flow. The radial velocity increases from 0 at the walls to 0.15m/s before decreasing to - 0.2m/s at the mid-centre for laminar flow while for turbulent flow the radial velocity intitially increases from 0 at the walls to 0.15m/s before decreasing to -0.06m/s at the discs centre; while for laminar flow, swirl velocity decrease from approximately 2.55m/s to 0.55m/s and for turbulent flow the swirl velocity decrease from approximately 2.84m/s to 1.62m/s. The turbulent flow swirl velocity profile seen to be smoother than for laminar flow around the discs centre. The study further showed that for fluid near the discs surfaces radial velocity net momentum is radially towards the outlet with flow laminar in the boundary layer region and the velocity turbulent towards the domain centre. For static pressure, laminar flow maximum and minimum static pressure 2.48pa and -0.033pa respectively, while for turbulent flow maximum and minimum static pressure were 0.00 and -0.0024pa.

     The developed previous study model can therefore be used to predict radial velocity distribution between steady axisymmetric flow between two parallel co-rotating discs.

Keywords-- Numerical Simulation, Radial Velocity, Axisymmetric Flow, Corotating Discs, Swirling Flow

I.   INTRODUCTION

Nikola Tesla's 1913 turbine patent is popularly referred to as bladeless turbine because the turbine rators are a set of smooth closely-spaced discs connected parallel to each other along a shaft. The bladeless turbine operates by the fluid spiralling from the inlet at the discs periphery inward towards the centre of the disc where it exits through the small hole near the disc centre. In the flow field, the fluid and discs interfaces are governed by the principle of centripetal force, viscou sand adhesion forces and boundary layer effects (Sengupta and Guha, 2012). In the case of a Tesla pump, the flow direction is reversed with the fluid entering through the small holes near the discs centre from where it spirals outwards towards the disc peripheral. In this case centrifugal forces come into play. Nevertheless, for both cases, as the fluid rotates within the rotating discs, it develops viscous drag in the boundary layer which in turns develops velocity gradient with gains in momentum (Schosser et al., 2016; Jose et al., 2016).

Tesla turbine, are not widely commercialized because of their low efficiency unlike Tesla pumps which are known to be commercially available since 1982 for abrasive, viscous, shear sensitive fluids, which contain solids. Presently, Tesla turbines find applications in power generation, vehicle technology whike the pump is in use as micro-polar pumps (Gupta and Kodali, 2013; Pandey et al., 2014).

The efficiency of Tesla turbines and pumps is known to depend on parameters such as pressure, temperature, inlet velocity, number of discs, discs gap, discs diameter, disc thickness, Reynolds number, angular velocity, disc surface finish, and fluid property. Because of its low efficiency problem their has been continued analytically, numerically and experimentally study of Tesla turbines (Gupta and Kodali, 2013).

With the introduction of the Tesla turbine patent, a lot of researches and studies have been undertaken in trying to overcome the low efficiency problem. Many, if not all, of these studies have resulted in analytical models that describe the flow between two discs in order to improve on the efficiency. In past studies, the values of parameters such as discs gap, radii ratio, number of discs and swirl ratio, on which efficiency depends are different for different investigator (Akpobi and Akele, 2015; Akpobi and Akele, 2016).

1.1 Governing Equations

The PDEs governing fluid flows are the known non-linear C-NS equations that completely describe the flow of incompressible, Newtonian fluids. The C-NS

equations being coupled and non-linear, their solutions by direct analytical manipulations are found to be formidable task to overcome. (Reddy, 1993). However, simple flows through parallel plates (e.g. Couette, Poiseuille, Couette-Poiseuille flows) are easily solved by applying two boundary conditions that will yield a closed-form of the C-NS equations. This later closed-form of the governing equations can then be solved by analytical or numerical methods. But in the case of complex flow problems (e.g. flows through rotating discs), these governing C-NS equations are usually simplified into a workable closed-form, notably by applying appropriate boundary conditions, order of magnitude analysis, and by the use of dimensionless parameters (Akpobi and Akele, 2016; Sengupta and Guha, 2012).

1.2 Galerkin Integral Finite Element Method

Finite element method (FEM) is a numerical technique for solving PDEs in which a continuous problem described by a differential equation is put into an equivalent variational form with approximate solution assumed to be a linear combination of approximation functions. One major advantage of FEM is that the techniques can divides complex geometric domain into sub-domains of arbitrary shape and size in order to enhance combination of different element shapes and computation of approximate solution. Thus, FEM provides approximations which are better closed-form when compared to those of other numerical methods. In finite element analyses (FEA), the inherent coupled and non-linearity problem of C-NS equations to flow problems are overcome by the use of the Galerkin weighted-residual integral approach that enables integration of the PDEs by parts (i.e. relaxing it) to form a 'weak' form of the equation and (ii) choice of approximation and interpolation functions (Reddy, 1993; Perumal and Amon, 2011).

1.3 Computational Fluid Dynamics (CFD)

The study of fluid flow between two rotating discs aims to predict flow characteristics. This attention on flow between two rotating discs aroused from the need to have comprehensive and detailed theoretical formulations that will aid in the design of the physical Tesla turbomachines for high efficiency. (Lopez, 1996).

II.   LITERATURE REVIEW

With the introduction of the Tesla turbine patent, a lot of researches and studies have been undertaken in trying to overcome the low efficiency problem. Many, if not all, of these studies have resulted in analytical models that describe the flow between two discs in order to improve on the efficiency. In past studies, the values of parameters such as discs gap, radii ratio, number of discs and swirl ratio, on which efficiency depends are different for different investigator (Akpobi and Akele, 2015; Akpobi and Akele, 2016).

Sengupta and Guha (2012) formulated a mathematical model on flow for turbine configuration.

The simplified closed-form equations were solved numerically using Lemma et al (2008) experimental data of r_1 = 13.2mm, r_2= 25mm, Ω = 1000rad/s, n_d = 9, Δp_{ic} = 0.113 bar for their geometry. Their results revealed that non-dimensional tangential velocity assumed parabolic profile between the discs, with tangential velocity increasing from the wall (v=0) to 1.5 at the two discs centreline, Non-dimensional radial velocity profile between the discs was observed to be parabolic and decreasing from 0 at the walls to -3 at the centreline. The specified inlet tangential velocity and radial velocity wrer 10.6m/s and -11.5m/s respectively. The Fluent results showed that tangential velocity increased with radius from 10.6m/s at the walls (for r = 1mm) to approximately 60 m/s at the midpoint (for r = 15mm). Their result also showed that pressure decreased from approximately 135 (at R = 0.528) to approximately 60 (at R = 1). Their maximum theoretical efficiency obtained was 21%; maximum power output of about 17.5 Watts at 3000rad/s was achieved at pressure drop between inlet and exit of Δp_{ic} = 0.113bar. Their work well agreed with Fluent 12 experimental results. Yu et al (2012) work was on theoretical analysis and experimental study of the pressure drop for radial inflow between co-rotating disks. The study revealed that centrifugal and Coriolis forces are the major factors that influenced the total pressure drop. That is with the influence of the centrifugal and Coriolis forces, the circumferential component of the absolute velocity can be very high resulting in pronounced total pressure drop in rotating cavity with radial inflow. The total pressure drop was observed to increase with flow-rate and Reynolds number. And at low Reynolds number, the total pressure drop was increased by the dimensionless mass flow-rate with the pressure increasing first before decreasing. Pandey et al. (2014) carried out a research study on the design and simulation analysis of 1 kW Tesla turbine in order to understand how it works. The study revealed that high efficiencies were only obtain at very low flow rates and the efficiencies are expected to be under 40%. Also, it was revealed that for higher pressure change, tangential velocities are higher with lower flow rates. The fluid model described by Allen (l990) was used for their CFD analysis. And fluid parameters of dimensional system constant R* was taken to be - 0.042 from which they judged their model to be acceptably accurate with obtained efficiency of 77.7%. Xing (2014) conducted direct numerical simulatiions in order to investigate Open von Karman swirling flow using two counterrotating coaxial discs enclosed in a cylindrical chamber with axial extraction. In the investigation, monotonic convergence was attained three grids that are symmetrically refined for average pressure at the disc outlet accompanied with small grid uncertainty of 3.5%. Circular vortices are reported to have formed with low discs rpm, rehardlesss of the flow rates; while with rpm between 300 and 500, negative spiral vortex is formed. Akpobi and Akele (2016) carried out numerical analysis to develop two dimensional rectangular elements models to predict velocity components and pressure

distributions in flow between two parallel co-rotating discs. The study revealed velocity components and pressure solutions to converged with exact solutions as the numbers of elements are increased with the initial inlet and no-slip boundary conditions well satisfied. Radial velocity was reported to increase from 0 at discs walls to maximum of 260 at domain centreline; while tangential velocity decreased from 0 at the walls to -1.05 at domain centreline. Radial velocity increases with radii ration from 0 at the disc gap centreline (inlet boundary) to maximum value of 16.23 at the disc outlet; tangential velocity decreases from 0 at the domain inlet centreline to -1.64 at the disc outlet and pressure increasing from 0 at the domain centreline inlet to 32.00 at the disc outlet. The work parametric study revealed that for different values of Reynolds number (Re), angular velocity (ω), swirl ratio (α), radii ratio (κ), maximum centreline velocity (U_{max}) radial velocity increases with increase in all the parameters within the disc gap. Whereas, for different values of Reynolds number (Re), angular velocity (ω), and radii ratio (κ) tangential velocity decreases with increase in all the parameters within the two discs domain; while for different values of swirl ratio (α), angular velocity (ω), maximum velocity (U_{max}) and radii ratio (κ) pressure increases from the disc inlet with increase in all the parameters.

III. METHODOLOGY

This study pump configuration is basically a swirling outflow configuration in which the fluid enters at an inlet near the discs centreline (r_i, z) with the outlet along the discs periphery (r_o, z). The fluid flow domain geometry is modelled in 2D cartesian coordinates with origin at O, the centreline between the two discs space, Fig. 3.1.
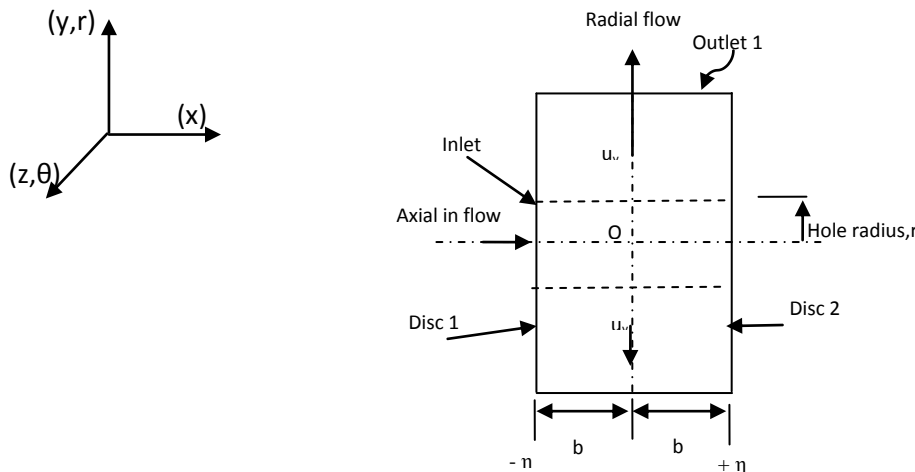
Fig. 3.1: 2D model geometry

3.1 Boundaries Geometry

The boundaries are set as in Fig. 3.2:
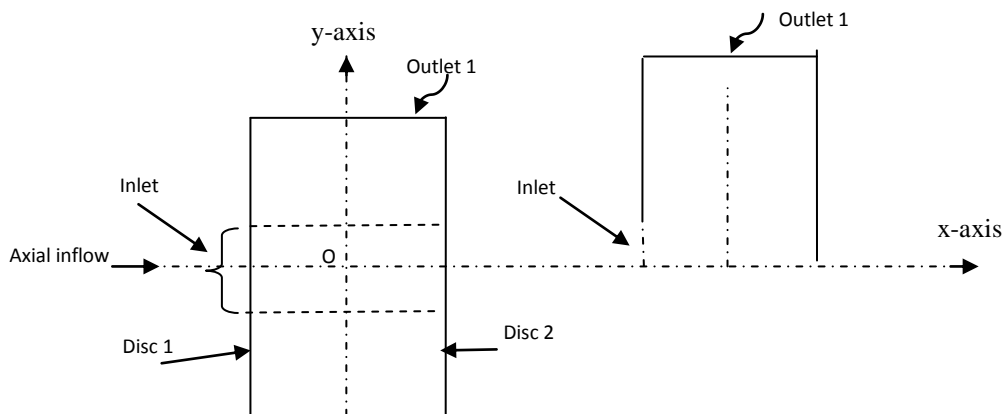
Fig. 3.2: boundary conditions

Considering the geometry of Fig 3.2, the fluid entering at the inlet (r_i, z) with initial uniform velocity ($v_i = 0$), comes in contact with both discs surface (solid) thus setting up velocity gradient in the boundary layer with no-slip boundary condition between disc-fluid interface, and with the viscous drag in the flow domain setting up a swirling radially outward flow in the fluid. The swirling pathlines on a rotating disc are as shown in Fig. 3.3 (Akpobi and Akele, 2016).
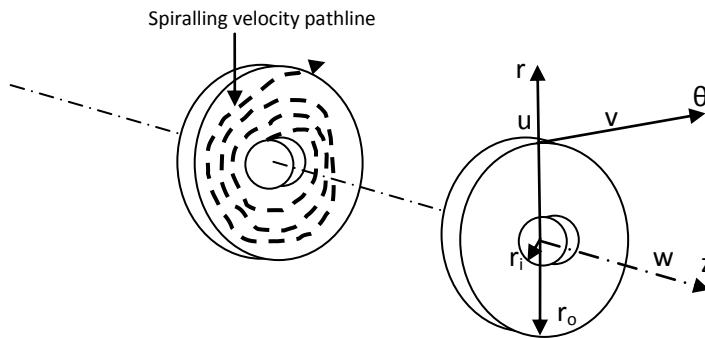
Fig 3.3: Swirling pathlines of outflow

3.2 Domain Discretization

For the analysis, quadrilateral elements are used since they are superior when compared to simple linear triangular elements in terms of meshing and accuracy of model meshing Perumal and Mon (2011). The domain Ω ($0 \leq \kappa \leq 1$; $-1 \leq \eta \leq +1$) is subdivided into quadrilateral elements mesh along the x- and y-axes respectively.

3.3 Governing Equations

For this research work, flow of fluid between the two discs is governed by the following C-NS equations (3.1), (3.2), (3.3) and (3.4) in Cartesian coordinates (Akpobi and Akele, 2015; Akpobi and Akele, 2016):

Continuity equation:

$$\frac{\partial \rho}{\partial t} + \frac{\partial (\rho u_x)}{\partial x} + \frac{\partial (\rho u_y)}{\partial y} + \frac{\partial (\rho u_z)}{\partial z} = 0 \tag{3.1}$$

x-momentum equation:

$$\rho \left(\frac{\partial u_x}{\partial t} + u_x \frac{\partial u_x}{\partial x} + u_y \frac{\partial u_x}{\partial y} + u_z \frac{\partial u_x}{\partial z} \right) = -\frac{\partial p}{\partial x} + \mu \left(\frac{\partial^2 u_x}{\partial x^2} + \frac{\partial^2 u_x}{\partial y^2} + \frac{\partial^2 u_x}{\partial z^2} \right) + \frac{1}{3} \mu \frac{\partial}{\partial x} \left(\frac{\partial u_x}{\partial x} + \frac{\partial u_y}{\partial y} + \frac{\partial u_z}{\partial z} \right) + \rho g_x \tag{3.2}$$

y-momentum equation:

$$\rho \left(\frac{\partial u_y}{\partial t} + u_x \frac{\partial u_y}{\partial x} + u_y \frac{\partial u_y}{\partial y} + u_z \frac{\partial u_y}{\partial z} \right) = -\frac{\partial p}{\partial y} + \mu \left(\frac{\partial^2 u_y}{\partial x^2} + \frac{\partial^2 u_y}{\partial y^2} + \frac{\partial^2 u_y}{\partial z^2} \right) + \frac{1}{3} \mu \frac{\partial}{\partial y} \left(\frac{\partial u_x}{\partial x} + \frac{\partial u_y}{\partial y} + \frac{\partial u_z}{\partial z} \right) + \rho g_y \tag{3.3}$$

z-momentum equation:

$$\rho \left(\frac{\partial u_z}{\partial t} + u_x \frac{\partial u_z}{\partial x} + u_y \frac{\partial u_z}{\partial y} + u_z \frac{\partial u_z}{\partial z} \right) = -\frac{\partial p}{\partial z} + \mu \left(\frac{\partial^2 u_z}{\partial x^2} + \frac{\partial^2 u_z}{\partial y^2} + \frac{\partial^2 u_z}{\partial z^2} \right) + \frac{1}{3} \mu \frac{\partial}{\partial z} \left(\frac{\partial u_x}{\partial x} + \frac{\partial u_y}{\partial y} + \frac{\partial u_z}{\partial z} \right) + \rho g_z \tag{3.4}$$

3.4 Relevant Assumptions

In order to simplify the non-linear C-NS equations (3.1) through (3.4) to workable level, the following assumptions are made (Akpobi and Akele, 2016):

(i)   flow is analysed in 2D,
(ii)   flow is in the radial direction and symmetrical over z-coordinate with very large discs radius and small gap, incompressible, steady, and viscous flow,
(iii)   flow in z-axis direction assumed insignificantly negligible,
(iv)   body forces (gravitational and inertia) are negligible,
(v)   no-slip condition exists at discs faces,

(vi)   both discs angular velocities are constant and equal.

At the discs hole inlet:
axial

$$v(-x_i, -y_i) = 0.2 m/s \qquad (3.5)$$

radial

$$u(x_i, 0) = 0$$

Static pressure at outlet:

$$p(y_o, x) = 0 \qquad (3.6)$$

At the two discs-fluid interfaces:

$$u(y, -x) = 0; u(y, +x) = 0 \qquad (3.7)$$
$$v(y, -x) = 0; v(y, +x) = 0,$$

At the discs walls:

$$D_1(y_o, -x) = D_2(y_o, +x) = \omega = 70 rpm \qquad (3.8)$$

3.6 Method of Solution

The method of solution used for simulation is ANSYS 16.2 CFD software. ANSYS Fluid Flow (Fluent) analysis system was used to draw the model geometry, generate the model quadrilateral meshes and then using the Fluent Solver to obtain the solutions. The 2D analysis was set up on 2D space, pressure-based, absolute velocity formulation, steady and axisymmetric swirling flow.

3.5 Boundary Conditions

The following boundary conditions are specified at the domain inlet, outlet and boundaries:

In this study, parameters from the CFD software are input into Akpobi and Akele (2016) developed radial velocity (dimensionless) model for flow between two discs to obtain dimensional radial velocity of the model. These input parameters, initial inlet and boundary conditions and disc geometry are shown in Table 1, Table 2 and Table 3 respectively.

Table 3.1: water properties

Water properties	
Density	$1000 kg/m^3$
Viscosity	$0.00089 N.s/m^2$
Temperature	300K
Pressure	1atm
Specific heat capacity	1006.43J/kg.K
Thermal conductivity	0.0242W/m.K
Molecular weight	28.966kg/kgmol

Table 3.2: initial and boundary conditions

Initial and Boundary conditions	
Axial Inlet velocity	0.20 m/s
Radial Inlet velocity	0 m/s
Outlet pressure	0 pa
Discs angular velocity	75rpm (7.85rad/s)
Swirl velocity	0rpm

Table 3.3: discs model geometry

Discs model geometry	
Number of nodes	2339
Disc diameter	100cm
Inlet hole diameter	4cm
Discs thickness	0cm
Discs gap	10cm

IV.   RESULTS AND DISCUSSION

The following table and figures show the results obtained.

Table 4.1: values of dimensionless (Akpobi and Akele, 2016) and dimensional (present study)

$(\kappa, \eta = 0)$	Akpobi and Akele (2015) (dimensionless)	This study (m/s)
0	0.0000000	0.00
0.125	0.0000561	517.46
0.250	0.0001048	965.92
0.333	0.0001460	1345.00
0.375	0.0001797	1656.00
0.500	0.0002059	1897.00
0.625	0.0002247	2070.00
0.667	0.0002359	2173.00
0.750	0.0002396	2208.00
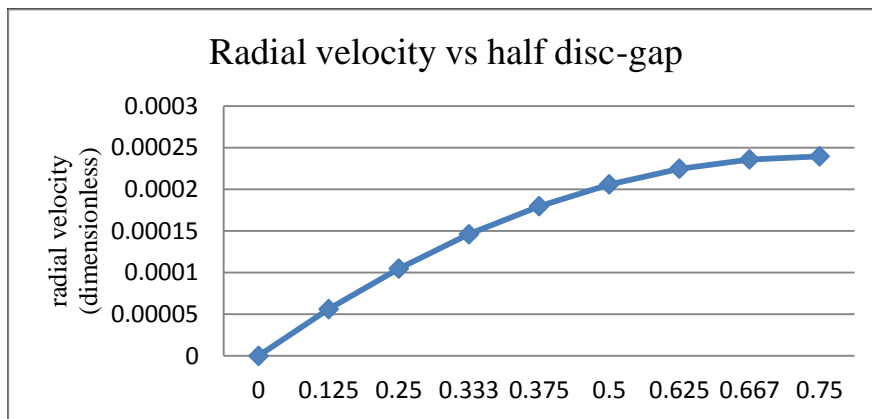
Fig. 4.1: dimensionless radial velocity
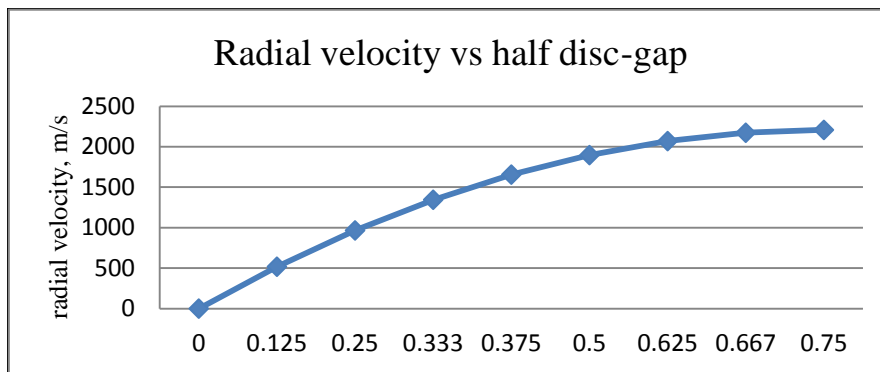
Fig. 4.2: dimensional radial velocity
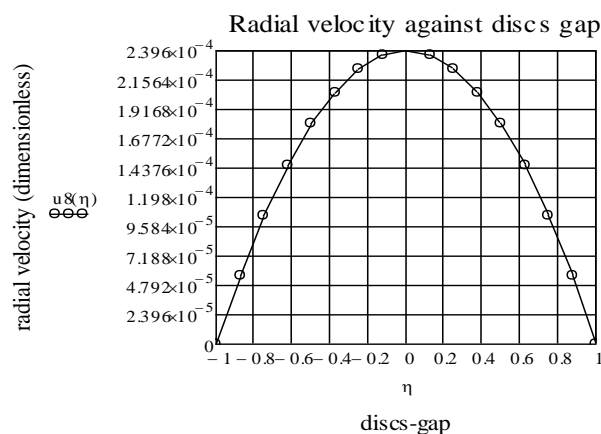
Fig. 4.3: dimensionless radial velocity distribution
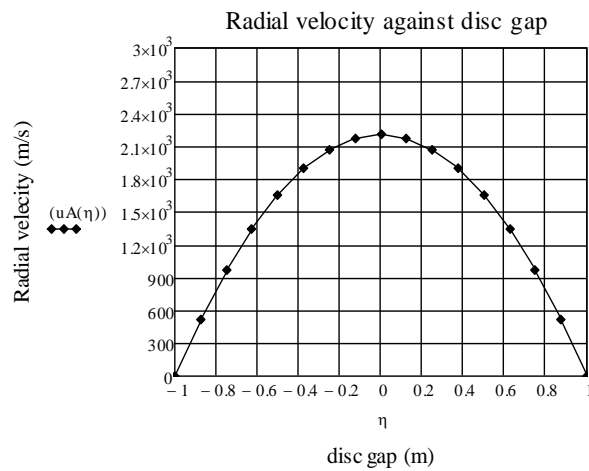
Fig. 4.4: dimensional radial velocity distribution
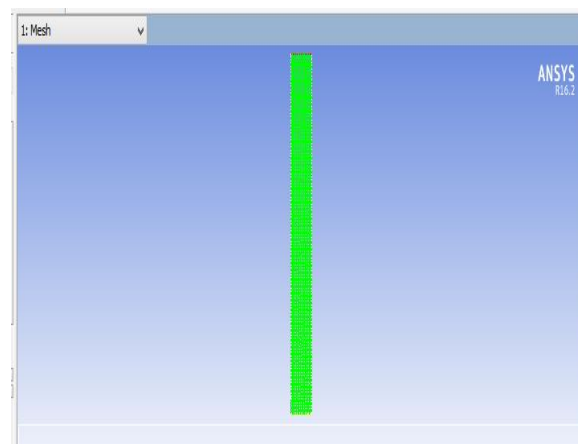
Fig 4.5: simulations mesh
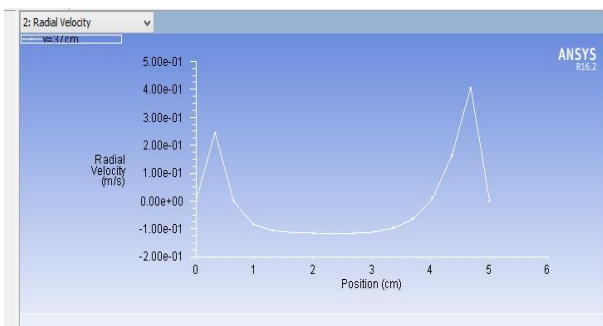
Fig 4.6: laminar radial velocity distribution
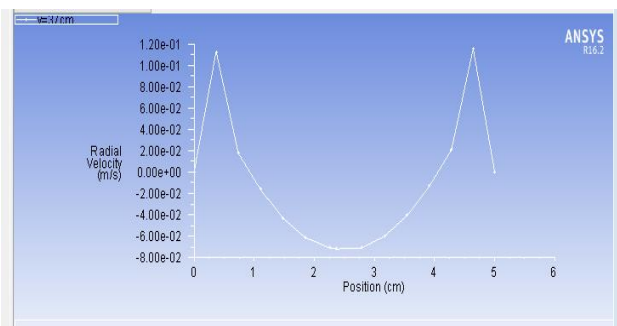
Fig 4.7: turbulent radial velocity distribution
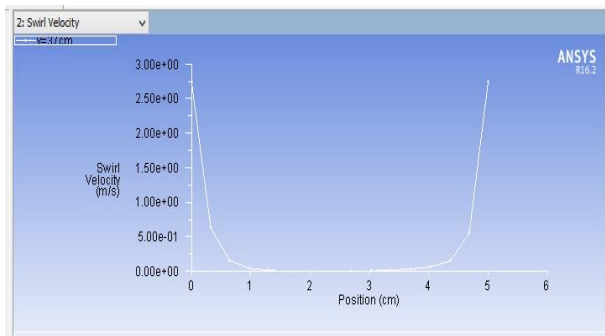
Fig 4.8: laminar flow swirl velocity   Fig 4.9: turbulent flow swirl velocity
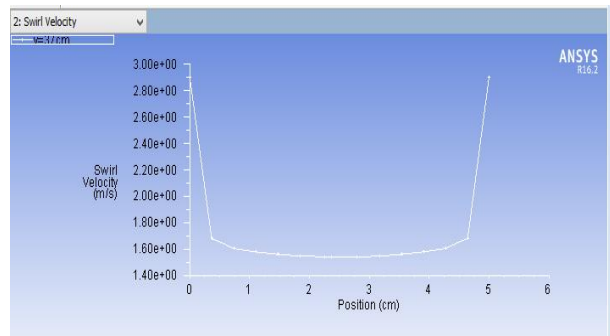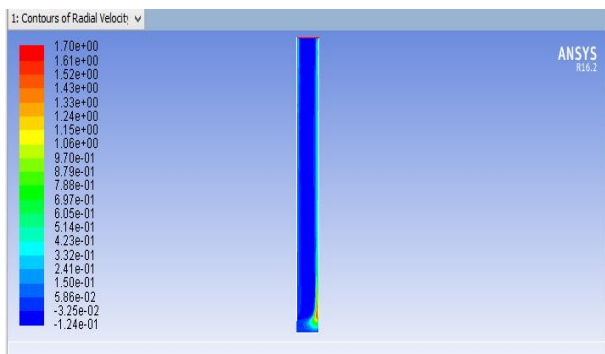
Fig 4.10: laminar flow contour of radial velocity   Fig 4.11: turbulent flow contour of radial velocity
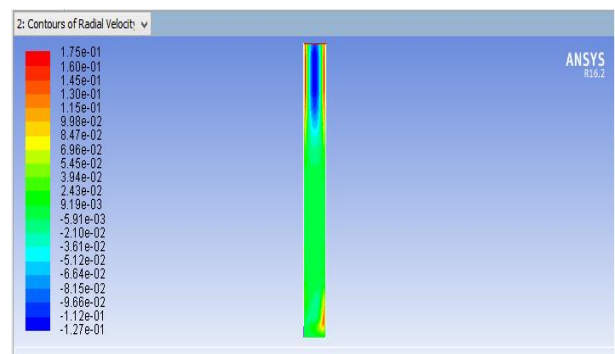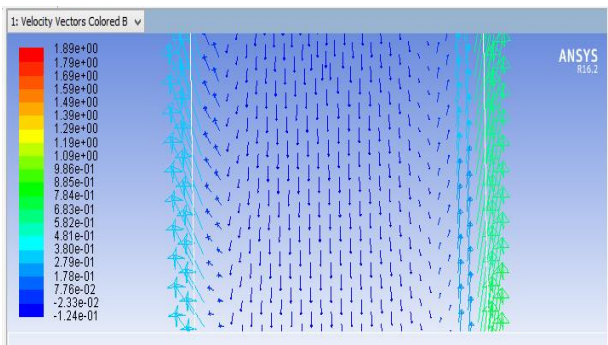
Fig 4.12: laminar flow velocity vector magnified   Fig 4.13: turbulent flow velocity vector magnified
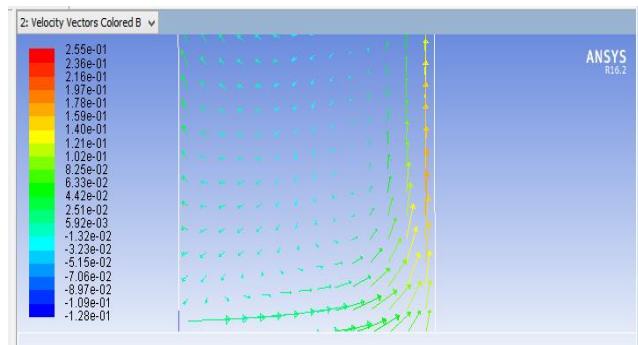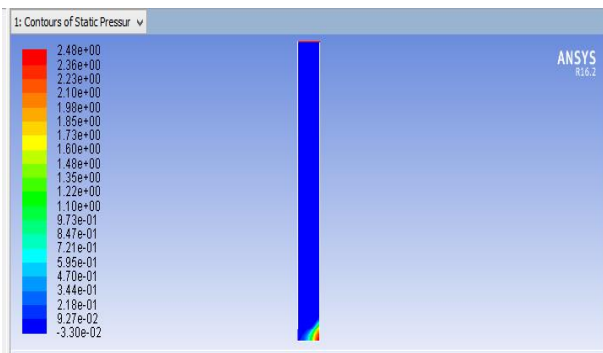
Fig 4.14: Laminar flow contour of static prssure   Fig 4.15: turbulent flow contour of static prssure
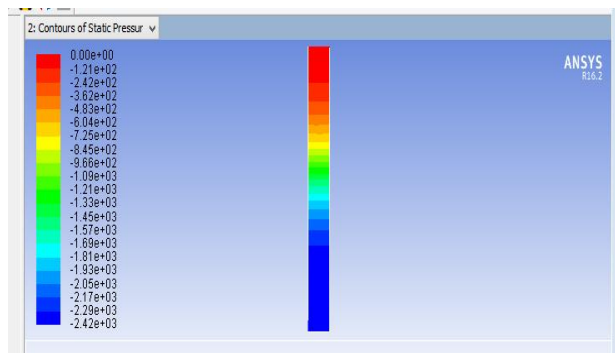
Table 4 shows the result obtained for dimensionless Akpobi and Akele (2016) and dimensional present study. The difference in values can be attributed to analysis inherent analytical errors, numerical computations errors, domain discretization errors and solution approximation errors of Galerkin integral finite element method used.

Fig. 4.1 and Fig. 4.2 are the dimensionless (Akpobi and Akele, 2016) and dimensional (present study) plots of radial velocity against half the disc gap (from one surface to the centre). Both distributions increase proportionately from the disc surface at 0 to the centre 0.0002396 (dimensionless) and 2208.00m/s respectively. While Fig. 4.3 and Fig. 4.4 are the dimensionless and dimensional plots of radial velocity over the flow domain (between the two discs surfaces) with minimum and maximum velocities of 0 and 0.0002396 (dimensionless) and 0 and 2208.00m/s respectively. And both curves satisfy initial inlet and boundary conditions with parabolic profile.

In Fig.4.6 and Fig 4.7, it is shown that turbulent flow radial velocity profile is smoother than for laminar flow. The radial velocity increases from 0 at the walls to 0.15m/s before decreasing to -0.2m/s at the mid-centre for laminar flow while for turbulent flow the radial velocity intitially increases from 0 at the walls to 0.15m/s before decreasing to -0.06m/s at the discs centre. Fig.4.8 and Fig 4.9 show laminar and turbulent flow swirl velocity distribution between the two discs. For laminar flow, Fig 4.8 shows that the swirl velocity decrease from approximately 2.55m/s to 0.55m/s; while for turbulent flow, Fig 4.9, the swirl velocity decrease from approximately 2.84m/s to 1.62m/s. The turbulent flow swirl velocity profile seen to be smoother than for laminar flow around the discs centre. In Fig.4.10 and Fig 4.11, it is shown that turbulent flow radial velocity profile is smoother than for laminar flow. The radial velocity increases from 0 at the walls to 0.15m/s before decreasing to -0.2m/s at the mid-centre for laminar flow while for turbulent flow the radial velocity intitially increases from 0 at the walls to 0.15m/s before decreasing to -0.06m/s at the discs centre. Fig. 4.12 and Fig. 4.13 show that for fluid near the discs surfaces radial velocity net momentum is radially towards the outlet. Fig. 4.12 show flow to be laminar in the boundary layer region while in Fig. 4 13 the velocity is shown be in turbulent, especially towards the domain centre.

In Fig. 4.14, laminar flow, maximum and minimum static pressure contour are shown respectively as 2.48pa and -0.033pa while for turbulent flow, Fig. 4.15, maximum and minimum static pressure contour are respectively 0.00 and -0.0024pa. For turbulent flow, stataic pressure is higher close to the outlet than for laminar flow.

V.   CONCLUSIONS

In this study, firstly, parameters from CFD software are input into Akpobi and Akele (2016) developed radial velocity (dimensionless) model for flow between two discs to obtain dimensional radial velocity of the model. Secondly, previous study parameters are used to perform numerical simulation on laminar and turbulent flows between two parallel co-rotating discs. The numerical simulation results are compared to previous study results. Comparative numerical simulations was carried out on laminar and turbulent flows using CFD software.

The results obtained show negligible difference in result obtained for this study simulation and previous study reslt. And the dimensionless previous study and this study dimensional radial velocity distributions both increase, proportionately, from the discs surfaces to the fluid flow domain centre while satisfying the initial inlet and boundary conditions.

The developed previous model can therefore be used to predict radial velocity distribution between steady axisymmetric flow between two parallel co-rotating discs.

RECOMMENDATIONS

For for study, a 3-dimension simulation be investigated. This ill allow for consideration of tangential velocity prediction along side radial velocity.

REFERENCES

[1] Akpobi, J. A. & Akele, SMG. (2015). Development of finite element models for predicting velocities and pressure distribution for viscous fluid flow between two parallel co-rotating discs. *International Journal of Engineering and Management Research, 5*(6), 724-742.

[2] Akpobi, J. A. & Akele, SMG. (2016). Development of 2D models for velocities and pressure distribution in viscous flow between two parallel co-rotating discs. *Journal of the Nigerian Association of Mathematical Physics, 2*, 233–290.

[3] Gupta, H. & Kodali, S. P. (2013). Design and operation of Tesla turbo-machine – A state of the art view. *International Journal of Advanced Transport Phenomena, 2*(1), 7-14.

[4] Jose, R., Jose, A., Benny, A., salus, A., & Benny, B. (2016). A theoretical study on surface finish, spacing between discs and performance of Tesla turbine. *International Advanced Research Journal in Science, Engineering and technology, 3*(3), 235-240.

[5] Lopez, J. M. (1996). Flow between a stationary and a rotating disc shrouded by a co-rotating cylinder. *Physics of Fluid, 8*(10), 2605-2613.

[6] Pandey, R. J., Pudasaini, S., Dhakal, S., Uprety, R. B., & Neopane, H. P. (2014). Design and computational analysis of 1kW Tesla Turbine. *International Journal of Scientific and Research Publications, 4*(11), 141-145.

[7] Perumal, L. & Mon, D. T. T. (2011). Finite elements for engineering analysis: A brief review. *International*

Conference on Modeling, Simulation and Control IPCSIT, 10, Singapore: IACSIT Press. Available at: www.ipcsit.com/vol10/12-ICMSC2011S034.

[8] Reddy, J. N. (1993). *An introduction to the finite element method*. (2nd ed.). New York: McGraw-Hill, Inc.

[9] Schosser, C., Lecheler, S., & Pfitzner, M. (2016). Analytical and numerical solutions of the rotor flow in Tesla turbine. Periodica *Polytechnica Mechanical Engineering, 61*(1), 12-22.

[10] Sengupta, S. & Guha, A. (2012). A theory of Tesla disc turbines. *Journal of Power and Energy, 266*(5), 650-663.

[11] Soong, C. (1996). Prandtl number effects on mixed convection between rotating coaxial discs. *International Journal of Rotating Machinery, 2*(3), 161-166.

[12] Xing, T. (2014). Direct numerical simulation of open von karman swirling flow. *Journal of Hydrodynamics, 26*(2), 165-177.

[13] Yu, X., Lu, H. Y., Sun, J. N., Luo, X., & Xu, G. Q. (2012). Study of the pressure drop for radial inflow between co-rotating disks. *28th International Congress of The Aeronautical Sciences*. Available at: https://academictree.org/sociology/publications.php?pid= 182803.